33RD INTERNATIONAL COSMIC RAY CONFERENCE, RIO DE JANEIRO 2013
THE ASTROPARTICLE PHYSICS CONFERENCE

ICRC 2013

The maximum momentum of the particles accelerated at interplanetary shock with free scattering probability

XIN WANG[1,2,3], NA WANG [1,2], YIHUA YAN[3]

[1] *Xinjiang Astronomical Observatory, Chinese Academy of Sciences, Urumqi 830011, China*
[2] *Key Laboratory of Radio Astronomy, Chinese Academy of Sciences, Nanjing 210008, China*
[3] *Key Laboratory of Solar Activities, National Astronomical Observatories, Chinese Academy of Sciences, Beijing 100012*

wangxin@xao.ac.cn

Abstract: The scattering time is an important factor which is connected with the maximum energy particle in the diffusive shock. In present simulations, the maximum momentum is calculated by allowing us to determine the scattering probability by scattering time in the scattering processes. We obtain the shape of the energy spectrum with cutoff at some maximum momentum. Also, we find that the value of the maximum energy particle would not increase as the scattering probability increases. This fact would imply that there would be a critical value of the scattering probability between the thermal mechanism and the non-thermal mechanism in the diffusive shock acceleration. Maybe it can explain the "break" characteristic of the energy spectrum observed from the spacecrafts.

Keywords: particle acceleration, shock wave, numerical simulation.

1 Introduction

Since the beginning of the investigations on the mechanism of particle acceleration at shock fronts, estimating the maximum energy of the accelerated particles has been one of the main goals, in the perspective of assessing the ability of the mechanism to explain the observed double power-law of the energy spectrum in solar cosmic rays. This issue has played a crucial role especially in the context of the so-called double-power law paradigm for the origin of solar energetic particle (SEP) events. In fact, it was understood very soon, in the case of interplanetary (IP) shocks, that acceleration would not keep the same efficient in the energy range from Mev to GeV in the modified shocks. The mechanism through which this generation of waves could occur was identified in the streaming instability [2] and widely discussed later by Ellison, Möbius & Paschmann [11]. In these latter papers, in particular, the maximum energy was estimated for IP shocks, already believed to be candidate sources of the SEP events. The result of this investigation was, however, that the maximum energy, even in the presence of self-generated scattering agents, is of the order of 1 MeV, quite near to the energy at which the "break" is observed[21, 24]. Today, we know that this energy is also lower than the maximum energy observed in the proton component by the spacecraft experiments that seems to be as high as 1 GeV [21].

Recently, the problem has been complicated even more by the understanding that particle acceleration can be rather efficient and break the test-particle regime that old calculations were based on [4]. This important result was obtained independently within completely different approaches, two-fluid models [7], kinetic models [1] and numerical approaches, using both Monte Carlo and other simulation procedures [11, 25]. The non-linear dynamical reaction of the accelerated particles introduces a positive reaction that results in a flattening of the high-energy spectra, which are no longer power laws, thereby enhancing the role of particles at the highest energies. Moreover, a gradient in the velocity of the upstream fluid is produced by the pressure of the accelerated particles. The value of p_{max} is important to determine the spectrum, and the spectrum determines the amplification of the magnetic field which in turn determines p_{max}. The formalism of Lagage & Cesarsky [18] is not appropriate to describe this type of situation. In this paper, we describe the calculation of the maximum momentum for solar cosmic ray in IP shocks with different dispersion of the scattering angular distribution, including a free scattering time in the scattering processes.

This paper is organized as follows. In Section 2, we describe the method that allows us to compute the maximum momentum as a function of the free scattering probabilities; in Section 3, we describe the procedure used to determine p_{max} in the case of varied scattering probability and discuss the underlying assumptions; in Section 4, we present the results for the maximum achievable momentum in IP shocks; finally, a summary of the main results and discussions are provided in Section 5.

2 Method

Since the prescribed scattering law in Monte Carlo model instead of the field calculation in hybrid simulations [13], we assume that particle scatters elastically according to a Gaussian distribution in the local plasma frame and that the mean free path (mfp) is proportional to the gyroradius (i.e., $\lambda \propto r_g$), where $r_g = pc/(qB)$, and its value is proportional to its momentum. Under the prescribed scattering law, the injection is purely correlated with those "thermal" particles which manage to diffuse back upstream fluid for obtaining additional energy gains and become superthermal particles [8].

The Monte Carlo model is a general model, and although it is rather expensive computationally, it is important in many applications owing to it including the dynamical effects of the non-linear diffusive shock acceleration(DSA). Since the prescribed scattering law can be used to replace calculation of the complex electromagnetic field in plasma simulations [13], we assume that the particles s-

catter elastically off the background scattering centers with their scattering angles following a Gaussian distribution in the local frame. In this scattering scenario, the assumption of elastic scattering requires that scattering centers are frozen into the background fluid [10]; simultaneously, the assumption of the constant scattering time for all particles means that the particle's mean free path is proportional to its local velocity in local frame with

$$\lambda = V_L \cdot \tau, \tag{1}$$

where τ is the average scattering time. These dependencies of the prescribed scattering law are similar to those in the hybrid simulation ($\lambda \propto v^{1/2}$)[9]. For the individual protons, the grid-based scattering center can be seen as a sum of individual momenta. So these scattering processes can be taken as the elastic collisions. In an increment of time, once all of the candidates complete these elastic collisions, the momentum of the grid-based scattering center is changed. In turn, the momentum of the grid-based scattering center will affect the momenta of the individual particles in their corresponding grid in the next increment time. The total simulation temporally evolves forward by repeating this time step sequence. To calculate the scattering processes accurately and produce an exponential mean free path distribution, the time step should be less than the scattering time (i.e. $dt < \tau$).

$$R_s = dt/\tau, \tag{2}$$

To model the finite size of the system and the lack of sufficient scattering far upstream to turn particles around, the presented simulation includes the escape of the energetic particles at an upstream "free escape boundary" (FEB). In the absence of a better description of this phenomenon (i.e. the difficulty from the technical point of view is that it is not clear which particles do actually escape the system), so far the best way to handle the escape flux is to impose a reasonable location for an FEB from the mathematical point of view [5]. As shown by Ellison, Möbius & Paschmann model[11], the bow shock is estimated to moved at a speed in the range of 10-100km s^{-1}. Given the time for the shock to happen $\sim$ 150s, one can figure out that the bow shock moved 1,500-15,000km. This distance was $\sim 40\lambda_0$, and thus λ_0=40-400km. The FEB distance in front of the shock was at $\sim$ -93λ_0, or between 0.5 and 5R_e from the shock. Since the FEB parameterizes the size of the acceleration region, our model assumes that the FEB distance in front of the shock at $\sim 3R_e$ can be plausible. Certainly, if not for computer constraints on the size of the simulation grid, a calculation with a substantially larger FEB (say, 100 times larger) would be more appropriate, but it is not feasible at this time. For investigate the different size of the FEB, we can choose the different scattering time in the diffusion processes instead of the effect on the maximum particle produced by different size of the FEB. Here we present the simulations having all the same parameters except for different scattering time in corresponding Cases. According to the basic scattering time τ_0, we chose the $\tau_0/2, \tau_0/4, \tau_0/3, \tau_0/4$ and $\tau_0/12.5$ for increasing the scattering probability allow to obtain the larger maximum momentum particles in several group of Cases. Accordingly, the scattering probabilities R_s are 4%,8%,12%,16%,20% and 50% in each group Cases, respectively.

The particle-in-cell techniques are applied in these dynamical Monte Carlo simulations. The simulation box is divided up into some number of cells and the field momentum is calculated at the center of each cell [12, 22]. The total size of a one-dimensional simulation box is set as X_{max} and it is divided into the number of grids N_{max}. Upstream bulk speed U_0 with an initial Maxwellian thermal velocity V_L in their local frame and the inflow in a "pre-inflow box" (PIB) are both moving along one-dimensional simulation box. The parallel magnetic field B_0 is along the $\hat{x}$ axis direction in the simulation box. A free escaped boundary (FEB) with a finite size (FEB=3R_e) in front of the shock position is used to decouple the escaped particles from the system as long as the accelerated particles beyond the position of the FEB. To obtain the information of the total particles in diffusion processes,we account the velocities and positions of all particles, as well as the index and the bulk speeds of all grids in each time step. The scattering angle distributions in each group Cases are presented by Gaussian distribution function with a standard deviation σ, and an average value μ involving three types of cases as three groups: (1) Case A: $\sigma = \pi/4$, $\mu = 0$. (2) Case B: $\sigma = \pi/2$, $\mu = 0$. (3) Case C: $\sigma = \pi$, $\mu = 0$. The specific parameters are described in detail in Wang & Yan model[23].

3 Calculation of P_{max}

In general, the value of p_{max} is determined by the competition between the acceleration time and the shortest among the finite age of the source, the time-scale for energy losses, and the time-scale for escape of particles with momentum p_{max} from upstream infinity. Here, we concentrate on the self-consistent calculation of the maximum momentum in those cases when it is determined by the assumption of scattering time or scattering probability. In such a context, each value of p_{max} therefore reflects a different scattering time τ of the system. In this sense, our previous work [23, 24] was based on the implicit assumption that a quasi-stationary system could be reached on time-scales of the scattering time of τ_0 in the diffusion processes, but no specific recipe for the calculation of p_{max} was adopted. In other work on non-linear diffusive particle acceleration at shock waves, p_{max} was either fixed or determined according to a simple recipe based on test-particle theory. Our determination of the maximum momentum proceeds through two different steps. (1)We first determine the dispersion of the scattering angular distribution σ for a given value of p_{max}; and then (2) we compare $R_s(p_{max})$ with the standard variation value σ of the scattering angular distribution in the diffusive system and determine an updated value of p_{max}. It is crucial to keep in mind that due to the non-linearity of the system, changing p_{max} causes the whole system to change (velocity profile, spectrum of accelerated particles, efficiency of particle acceleration and also the diffusion coefficient, if the scattering is due to self-generated waves). The results obtained by applying this procedure are illustrated in the next section.

4 Results

4.1 The Maximum Momentum Function

Following the method outlined in Section 2, we computed the maximum momentum of the accelerated particles as a function of the scattering probability, under different assumptions on the dispersion of the scattering angular distribution. The calculated results of the three group's

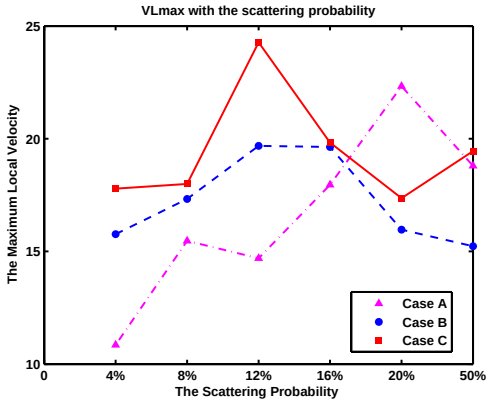

Fig. 1: The maximum momentum curves as a function of the scattering probability in three group of cases: Cases A, $\sigma = \pi/4$, Cases B, $\sigma = \pi/2$, Cases C, $\sigma = \pi$, where σ is the standard value of the scattering angular distribution.

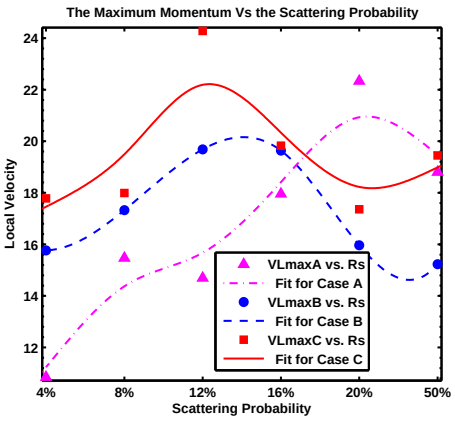

Fig. 2: The fitting curves of the maximum momentum as a function of the scattering probability in three group of cases: Cases A, Cases B, and Cases C with different dispersion of the scattering angular distribution.

maximum momentum are summarized in Fig.1. The dot-dashed, dashed, and solid lines denoted the maximum momentum of the accelerated particles vs the scattering probabilities, namely with self-generated scattering in Cases A, Cases B and Cases C, respectively. We assumed an Earth bow shock formation and considered the scattering time τ ranging from τ_0, $\tau_0/2$, $\tau_0/3$, $\tau_0/4$, and $\tau_0/5$ to $\tau_0/12.5$. In the first panel of the Fig.1, the marks of triangle, circle, and square are represented the maximum particles at the corresponding scattering time τ in three groups. In the Fig.2, we show the fitting curves of the maximum momentum of the accelerated particles as the function of the scattering probability in three different dispersion of the scattering angular distributions. The maximum momentum are calculated from our simulations can be seen as the intersection with the shock formation time for T_{total}=6.3 minutes, assumed to be the time of the shock system evolution. Each fitting curve in the Fig. 2 shows a peak value of the maximum momentum at a certain scattering probability. The dot-dashed line, dashed line, and solid line are fit for the p_{max} data of three groups of Cases A, Cases B, and Cases C,respectively. As shown in the Fig. 2, the maximum momentum functions with their peak values of the p_{max} located in different scattering probabilities from Case A, and Case B to Case C, respectively. The corresponding scattering probability are correspond to a decreasing value of Rs=20%, Rs=14% and Rs=12%from Case A, and Case B to Case C, respectively. The critical peak value of the maximum momentum with its scattering probability in Cases C fits the observations from the multiple spacecrafts as shown in previous paper [24]. The maximum achievable momentum as a function of scattering probability, produce different critical point of the scattering probability. When the scattering probability is larger than this critical value of the scattering probability, the maximum achievable momentum will not increase as the scattering probability. This means that the acceleration efficiency become lower relatively. It just imply that the non-thermal mechanism transferred to the thermal mechanism over the critic scattering probability in the diffusive plasma.

4.2 Energy Spectrum

Still the comparison between the three panels allows to highlight what the main effect of the different dispersion of anisotropic angular distribution is: in the case of strongly anisotropic scattering in the pitch angle distribution, the spectra become very soft at high energies as discussed in detail elsewhere [23, 24]. This is the reason for the behaviour of scattering probability observed in the left panel, which may seem similar shape at first sight for the slope of the curves referring to scattering probability R_s from 4%, 8%, 12%, 16%, and 20% to 50%; in the case of strongly isotropic scattering in the pitch angle distribution, the spectra become very hard at high energy range. This is the reason for the behaviour of scattering probability observed in the right panel, which may seem dispersive shape at first sight for the slope of the curves referring to scattering probability R_s from 4%, 8%, 12%, 16%, and 20% to 50%. By comparing three panels, it is clear that things change drastically, with the dependence of critical value of the maximum momentum of the accelerated particles on dispersion of the scattering angular distributions becoming much stronger. Finally, let us discuss the behaviour of the maximum achievable momentum as a function of the scattering probability. This latter fact is clearly related to the more strongly modified velocity profile that leads to lower and lower values of the flow velocity in the vicinity of the shock and as a consequence increasingly longer residence times upstream. The dependence of the maximum achievable momentum on the scattering probability is illustrated more clearly in Fig. 3, where we plot the cut off of the p_{max} as a function of scattering probability for three different dispersion of scattering angular distribution. The left panel represents Case A, the dotted line shows the flattest spectrum at the scattering probability $Rs = 20\%$; the middle panel represents Case B, the solid line shows the flattest spectrum at the scattering probability $Rs = 16\%$; the right panel represents Case C, the dot-dashed line shows the flattest spectrum at the scattering probability $Rs = 12\%$. This is illustrated effectively through the energy spectra in Fig. 3, where the cut-off of the p_{max} are calculated with different scattering probabilities in each group of cases, assumed constant in the precursor. In these cases, the value of p_{max} is always near a few MeV for all the given scat-

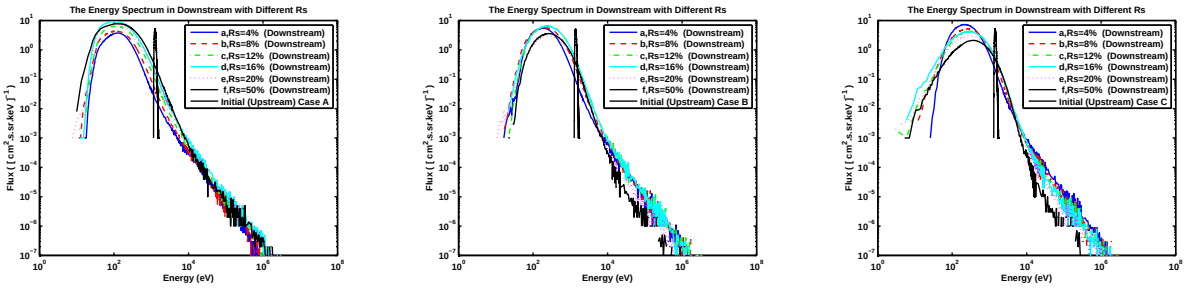

Fig. 3: Three panels from the left to the right represent the energy spectrum at six given scattering probabilities in three group of cases: Cases A, Cases B, and Cases C, respectively. The variation of the high energy spectrum in the left panel show a little differences; however, in the right panel, the variation of the high energy spectrum shows a largely differences, relatively. The middle panel, the variation of the high energy spectrum shows a middle differences, correspondingly.

tering probability $> 4\%$. We have not obtained $p_{max} > 10$ MeV, although we expect to obtain the cut-off of p_{max} up to 10 MeV and above. In the presence of the large times of size of the FEB in front of the modified shock, we expect to get the value of p_{max} near the energy range from ~ 10 MeV to GeV.

5 Conclusions

In this section, we summarize the reasons for the need of the type of calculations presented here. We calculated the maximum momentum of the particles accelerated at a cosmic ray modified shock, where the non-linear dynamical reaction of the accelerated particles changes the shocked fluid, the particles self-generate their own scattering centers. The size of a shock precursor in the upstream region are the main reasons to expect that the maximum achievable momentum may be appreciably determined. For the constraint of the computation, we have investigated the maximum achievable momentum as a function of the scattering probabilities. We find the cut-off of the maximum momentum increases as the scattering probability up to the critical scattering probability, then does not increase as the scattering probability increases. Also we find that the critical scattering probability has a different values in different dispersion of the scattering angular distribution. The stronger anisotropy in the pitch angle scattering processes, the larger value of the critical scattering probability is occur. It may imply that there exist a critical point of the non-thermal mechanism and thermal mechanism corresponding to the critical scattering probability and the "break" of the power-law spectrum.

Acknowledgment: This paper is funded by CAS-NSFC grant 10778605 and NSFC grant 10921303 and the National Basic Research Program of the MOST (Grant No. 2011CB811401). In addition, this work is also supported by Xinjiang Natural Science Foundation No. 2009211B35, the key Directional Project of CAS and NNSFC under the project No. 10173020, No. 0673021 and Chinese National Science Foundation through grant No. 10573005.

References

[1] Amato E., Blasi P., MNRAS, 2006, 371, 1251
[2] Bell, A.R., MNRAS, 1978, **182**: 147
[3] Blasi, P., Gabici, S., & Vannoni, G., MNRAS, 2005, **361**: 907
[4] Blasi,P., Amato,E. & Caprioli, D., 2007, MNRAS, 2007, **375**: 1471
[5] Caprioli, D., Blasi,P. & Amato,E. 2010, Astropart. Phys., 33, 307
[6] Caprioli, D., Kang, H., Vladimirov, A. E.,*et al.* , MNRAS, 2010, **407**: 1773
[7] Drury L. OC., Völk H. J., ApJ, 1981, 248, 344
[8] Ellison, D. C., Blasi & Gabici , 2005, in Proc. 29th Int. Comsmic Ray Conf. (India).
[9] Ellison, D. C., Giacalone, J. , Burgess, D. & Schwartz,S. J. 1993, JGR, 98,21085
[10] Ellison, D. C. & Double,G. P. 2004, Astropart. Phys., 22, 323
[11] Ellison, D. C., Möbius, E. & Paschmann, G. 1990, APJ, **352**: 376
[12] Forslund, D. W., SSR, 1990, **42**: 3
[13] Giacalone, J. , A&A, 2004, **609**: 452
[14] Gosling, J.T., Asbridge, J.R., Bame, S.J., *et al.* , JGR, 1981, **866**: 547
[15] Kang H. & Jones T.W., A. Ph., 2007, **28**: 232
[16] Knerr, J. M., Jokipii, J. R. & Ellison, D. C., APJ, 1996, **458**: 641
[17] Lee, M. A., APJS, 2005, **158**: 38
[18] Lagage P. O., Cesarsky C. J., A&A, 1983, 118, 223
[19] Li, G., Zank, G.P., & Rice, W.K.M., JGR, 2003, **108**: 1082
[20] Pelletier, G., LNP, 2001, **576**: 58
[21] Mewaldt, R. A., Cohen, C. M. S., Cummings, A. C., et al. 2008, 30th International Cosmic Ray Conference, Int. Union of Pure and Appl. Phys., Mrida, Mexico. Vol.1 (SH) 107-110.
[22] Niemiec, J., Pohl, M., Stroman, T., *et al.* , APJ, 2008, **684**: 1174
[23] Wang, X., & Yan, Y., A&A, 2011, **530**: A92
[24] Wang, X. & Yan, Y. 2012, Research in Astronomy and Astrophysics 12, 1535-1548
[25] Vladimirov A., Ellison D. C., Bykov A., ApJ, 2006, 652, 1246